Understanding the Physical Degrees of Freedom in a Parameterized Test of General Relativity

Leif Lui
Department of Physics, The Chinese University of Hong Kong, Sha Tin, NT, Hong Kong

Mentors: Rico K. L. Lo and Alan J. Weinstein
LIGO, California Institute of Technology, Pasadena, California 91125, USA
(Dated: June 15, 2021)

The following is a proposal that provides a framework for understanding the physical degrees of freedom in a parameterized test of general relativity. In particular, we vary the post-Newtonian (PN) coefficient, phenomenological coefficients, and the analytical black-hole perturbation theory waveform parameters, and observe how this would affect the waveform and hence the physical parameters. The physical parameters include the power radiated and the rate of angular momentum. Although it is possible to map the dephasing coefficient to physical quantities, the inverse mapping of the physical quantities to the dephasing coefficients is unknown. Therefore, this proposal presents a method of obtaining this inverse mapping using the Gaussian Mixture Model (GMM).

I. INTRODUCTION

The detection of gravitational waves (GWs) by the Advanced LIGO and Virgo [1–11] has opened new windows in observational astrophysics and cosmology. More specifically, it stands to test the limits of Einstein's theory of general relativity (GR). More recent work has been focused on testing GR in the strong-field/highly-relativistic regime. Such test could potentially reconcile the deviations of GR with quantum field theory, through examining the higher-energy corrections to the Einstein-Hilbert action [12].

Of the many strong-field astrophysical events, this proposal focuses on the coalescence of binary black holes (BBHs). This is because, firstly, the gravitational fields generated can be many orders of magnitude stronger than any other astrophysical events, as the BBHs' orbital separation can be smaller than the last stable orbit before merging. Secondly, BBH coalescence gives one of the cleanest signals for testing GR, as it is separated into three distinct phases: the inspiral, merger, and ringdown (IMR) phases [13].

A parametrized test is, simply put, a test where one measures the deviation of some parameters from their GR predictions. For parameterized tests of GR, the phenomenological models are most ideal, as they have a closed-form expression in the frequency domain and hence can be more computationally efficient. In particular, we focus on doing a parameterized test of GR on `IMRPhenomPv2` [14–17]. `IMRPhenomPv2` is a waveform model that approximates a signal of a precessing binary. It is used because it has good performance across the parameter space [15]. The purpose of the parameterized test is to understand the physical significance of varying the dephasing coefficients in the waveform and see whether such changes have deviations from GR.

Throughout the entirety of this proposal, the geometric unit convention is adopted, where $c = G = 1$.

II. PARAMETERIZED TEST OF GR

As mentioned in the Section I, a parameterized test of GR is to search for digressions of observations from the predictions of GR. To perform the parameterized tests, we introduce fractional deviations δp_i to the `IMRPhenomPv2` phase coefficients p_i [18], namely

$$p_i \to (1 + \delta p_i) p_i. \tag{1}$$

These fractional deviations are known as the dephasing coefficients. The phasing of `IMRPhenomPv2` consists of three regimes. The first of which is the inspiral regime which is parameterized by post-Newtonian (PN) coefficients [19] $\{\varphi_0, \ldots, \varphi_7\}$ and $\{\varphi_{5l}, \varphi_{6l}\}$. In this regime, there are also phenomenological parameters $\{\sigma_0, \ldots, \sigma_4\}$ that contribute to the high effective PN order. This corrects for non-adiabaticity in the late inspiral phase and for unknown high-order PN coefficients in the adiabatic regime. The second regime, is the intermediate regime, which is parameterized by the phenomenological coefficients $\{\beta_0, \ldots, \beta_3\}$. Finally, there is the merger-ringdown regime which is parameterized by a combination of the phenomenological coefficients and the analytical black-hole perturbation theory parameters $\{\alpha_0, \ldots, \alpha_5\}$ [13]. As one can see if $\delta p_i = 0$ this corresponds to a theory with no deviation with GR.

In FIG. 1, we have the phase evolution of an `IMRPhenomPv2` waveform with varied dephasing coefficient. A dephasing coefficient is chosen from each regime to illustrate how the dephasing coefficient changes the waveform and hence the physical parameters. More specifically, FIG. 1 illustrates how the dephasing coefficient changes the phase. In FIG. 2, we change the same dephasing coefficients as those in FIG. 1, however this time we plotted the strain data. This illustrates how the dephasing coefficient actually changes the shape of the GW waveform.

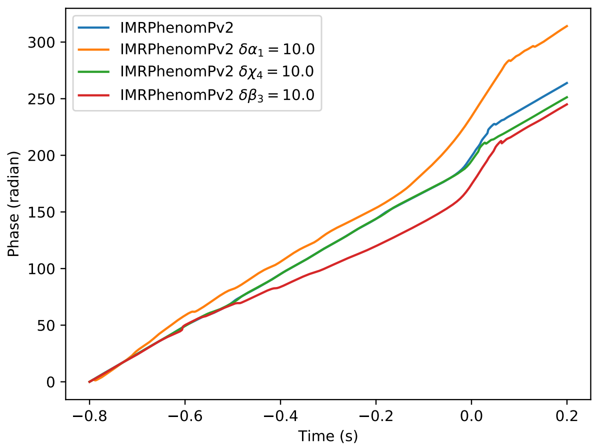

FIG. 1. Phase of GW versus time for `IMRPhenomPv2` with no modification (blue line), $\delta\alpha_2 = 10.0$ (orange line), $\delta\chi_4 = 10.0$ (green line), and $\delta\beta_3 = 10.0$ (red line). Here it can be seen that the change in dephasing coefficient alters the phase of the waveform over time.

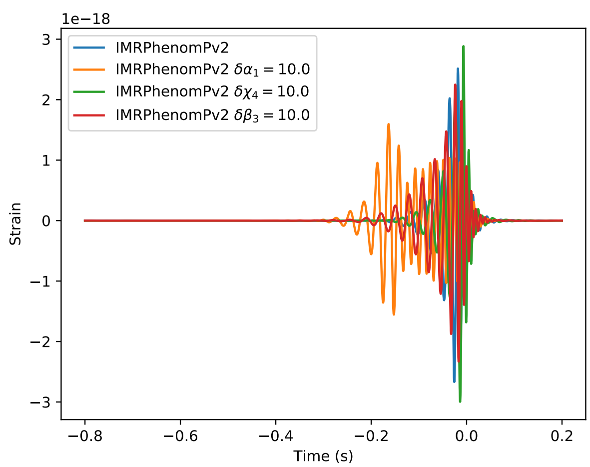

FIG. 2. Strain versus time for `IMRPhenomPv2` with no modification (blue line), $\delta\alpha_2 = 10.0$ (orange line), $\delta\chi_4 = 10.0$ (green line), and $\delta\beta_3 = 10.0$ (red line). One can see the change in shape of waveform when plotting the strain data.

Throughout the entirety of this project, we will use the parameterized test of TIGER (Test Infrastructure for GEneral Relativity) [20, 21]. This infrastructure is prevalent, as it does not require an alternative theory of gravity to compare against. In addition to this, TIGER is dependent on the measurement of parameterizable deviations, like the aforementioned deviation in dephasing coefficients from a GR-consistent waveform model.

Let $\mathcal{H}_{\rm GR}$ be the hypothesis that some GW signal h is consistent with GR. To test how this hypothesis deviates from GR, we introduce another hypothesis $\mathcal{H}_{\rm MG}$ (MG stands for modified gravity) which is a hypothesis that the waveform model differs by one or more dephasing coefficient. Since $\mathcal{H}_{\rm GR}$ and $\mathcal{H}_{\rm MG}$ are mutually exclusive, and given some data d and information I, we can define the Bayes factor [13]

$$\mathcal{B} = \frac{p(d|\mathcal{H}_{\rm MG}, I)}{p(d|\mathcal{H}_{\rm GR}, I)}, \tag{2}$$

where $p(d|\mathcal{H}_{\rm GR}, I)$ and $p(d|\mathcal{H}_{\rm MG}, I)$ are the posterior probability densities of the data given hypothesis $\mathcal{H}_{\rm GR}$ and $\mathcal{H}_{\rm MG}$, respectively. If $\log\mathcal{B} > 0$, then the hypothesis $\mathcal{H}_{\rm MG}$ is favored, on the other hand if $\log\mathcal{B} < 0$ the hypothesis $\mathcal{H}_{\rm GR}$ is preferred [22]. Hence, we have a quantitative way of determining whether a waveform deviates from GR. This can be computed using some Bayesian inference libraries like `bilby` [23] or `LALInference` [24, 25].

III. PARAMETER ESTIMATION

In Ref. [13], the Bayesian statistics framework is used to do parameter estimation. In such framework, the posterior distribution for some parameter λ is [13, 24, 25]

$$p(\lambda|\mathcal{H}_i, d, I) = \frac{p(\lambda|\mathcal{H}_i, I)p(d|\mathcal{H}_i, \lambda, I)}{p(d|I)}, \tag{3}$$

where $\mathcal{H}_i$ is the hypothesis that corresponds to a waveform model in which δp_i is a free parameter. In the equation above, d is the data, I is the background information, $p(\lambda|\mathcal{H}_i, I)$ is the prior probability density for the free parameters, and $p(d|\mathcal{H}_i, \lambda, I)$ is the probability of the data. $p(d|\mathcal{H}_i, \lambda, I)$ is defined as the likelihood function, which can be written as [13, 24, 25]

$$p(d|\mathcal{H}_i, \lambda, I) \propto e^{-\frac{1}{2}\langle d-h(\lambda)|d-h(\lambda)\rangle}, \tag{4}$$

where $h(\lambda)$ is the signal model and the inner product is defined as [13]

$$\langle a|b\rangle = 4\Re\int_{f_{\rm low}}^{f_{\rm high}} {\rm d}f\,\frac{a^*(f)b(f)}{S_n(f)}. \tag{5}$$

In Eq. (5), $f_{\rm high}$ is the high-frequency cutoff and $f_{\rm low}$ is the low-frequency cutoff. In the equation above, $S_n(f)$ is the power spectral density of noise. To obtain the posterior density for parameter δp_i, one has to marginalize over all parameters other than δp_i. These are also known as the nuisance parameters.

$$p(\delta p|\mathcal{H}_i, d, I) = \int {\rm d}\vec{\theta}\, p(\vec{\theta}, \delta p_i|\mathcal{H}_i, d, I), \tag{6}$$

where the integration is carried out over all nuisance parameters.

IV. RATES OF ENERGY AND ANGULAR MOMENTUM OF GWS

The physical parameters that we are interested in are the rates of energy and angular momentum. We can compute the energy and momentum using the Isaacson stress-energy tensor [26, 27]

$$t_{\mu\nu} = -\frac{1}{8\pi}\left\langle R^{(2)}_{\mu\nu} - \frac{1}{2}\bar{g}_{\mu\nu}R^{(2)}\right\rangle, \tag{7}$$

where $R^{(2)}_{\mu\nu}$ is the Ricci tensor to quadratic order. $R^{(2)}_{\mu\nu}$ usually involves many terms quadratic in the metric perturbation, however we can drastically simplify this expression by performing integration by parts and using the transverse-traceless (TT) gauge condition

$$R^{(2)}_{\mu\nu} = -\frac{1}{4}\left\langle \partial_\mu h_{\alpha\beta}\partial_\nu h^{\alpha\beta}\right\rangle. \tag{8}$$

Therefore the Isaacson stress-energy tensor can be written explicitly as

$$t_{\mu\nu} = \frac{1}{32\pi}\left\langle \partial_\mu h^{\mathrm{TT}}_{\alpha\beta}\partial_\nu h^{\alpha\beta}_{\mathrm{TT}}\right\rangle \tag{9}$$

To compute the energy carried by a GW, we take the 00-component of the Isaacson stress-energy tensor and integrate over the volume V[26, 27]

$$\frac{\mathrm{d}E}{\mathrm{d}t} = \frac{1}{16\pi}\int_S \mathrm{d}\Omega\, r^2\left\langle \dot{h}^2_+ + \dot{h}^2_\times\right\rangle, \tag{10}$$

where h_+ and $h_\times$ are the plus and cross polarizations of the GW, respectively. The overhead dot in Eq. (10) is the derivative with respect to coordinate time. Another useful expression is the energy spectrum, as it is much easier to integrate over all frequency

$$\frac{\mathrm{d}E}{\mathrm{d}f} = \frac{\pi}{2}f^2\int_S \mathrm{d}\Omega\, r^2\left(|\tilde{h}_+(f)|^2 + |\tilde{h}_\times(f)|^2\right). \tag{11}$$

On the other hand, to compute the rate of angular momentum, we compute the linear momentum and take the cross product with the separation vector. The linear momentum is as follows[26, 27]

$$\frac{\mathrm{d}P_i}{\mathrm{d}t} = \frac{1}{32\pi}\int \mathrm{d}\Omega\, r^2\left\langle \dot{h}^{\mathrm{TT}}_{ij}\partial^k \dot{h}^{\mathrm{TT}}_{ij}\right\rangle. \tag{12}$$

Therefore, the total rate of change in angular momentum carried by the GWs can be written as

$$J^i = \frac{1}{2}\epsilon^{ijk}J_{kl}, \tag{13}$$

where J_{kl} is the conserved charge associated with rotation in the $kl-$plane. Using Noether's theorem, we find that the expression for rate of angular momentum is as follows[26, 27]

$$\frac{\mathrm{d}J_i}{\mathrm{d}t} = \frac{1}{32\pi}\int_S \mathrm{d}\Omega\, r^2\langle -\epsilon^{ikl}\dot{h}^{\mathrm{TT}}_{ab}x^k\partial^l h^{\mathrm{TT}}_{ab} + 2\epsilon^{ikl}\dot{h}^{\mathrm{TT}}_{al}h^{\mathrm{TT}}_{ak}\rangle. \tag{14}$$

To carry out the integration numerically, multipole expansion is performed on the rates of energy and angular momentum[27].

V. TIMELINE

- 1st-2nd week: Calculate the energy/angular momentum of the inspiral part.
- 2nd-3rd week: Writing, plotting, and analyzing the results, along with writing the first interim report.
- 4th-5th week: Perform the energy calculations but for the post-inspiral and merger-ringdown part.
- 5th-7th week: Calculation of the angular momentum of the entire waveform.
- 7th-8th week: Learn the statistics of the Gaussian Mixture Model (GMM).
- 9th-10th week: Perform TIGER run and prepare for final presentation.

[1] B. P. Abbott *et al.* (LIGO Scientific Collaboration and Virgo Collaboration), Observation of gravitational waves from a binary black hole merger, Phys. Rev. Lett. **116**, 061102 (2016).

[2] B. P. Abbott *et al.* (LIGO Scientific Collaboration and Virgo Collaboration), GW151226: Observation of gravitational waves from a 22-solar-mass binary black hole coalescence, Phys. Rev. Lett. **116**, 241103 (2016).

[3] B. P. Abbott *et al.* (LIGO Scientific and Virgo Collaboration), GW170104: Observation of a 50-solar-mass binary black hole coalescence at redshift 0.2, Phys. Rev. Lett. **118**, 221101 (2017).

[4] B. P. Abbott *et al.*, GW170608: Observation of a 19 solar-mass binary black hole coalescence, The Astrophysical Journal **851**, L35 (2017).

[5] B. P. Abbott *et al.* (LIGO Scientific Collaboration and Virgo Collaboration), GW170814: A three-detector observation of gravitational waves from a binary black hole coalescence, Phys. Rev. Lett. **119**, 141101 (2017).

[6] B. P. Abbott *et al.* (LIGO Scientific Collaboration and Virgo Collaboration), GW170817: Observation of gravitational waves from a binary neutron star inspiral, Phys. Rev. Lett. **119**, 161101 (2017).

[7] B. P. Abbott *et al.* (LIGO Scientific Collaboration and Virgo Collaboration), GWTC-1: A gravitational-wave transient catalog of compact binary mergers observed by

ligo and virgo during the first and second observing runs, Phys. Rev. X **9**, 031040 (2019).

[8] R. Abbott *et al.* (LIGO Scientific Collaboration and Virgo Collaboration), GW190412: Observation of a binary-black-hole coalescence with asymmetric masses, Phys. Rev. D **102**, 043015 (2020).

[9] B. P. Abbott *et al.*, GW190425: Observation of a compact binary coalescence with total mass ~ 3.4 m $\odot$, The Astrophysical Journal **892**, L3 (2020).

[10] R. Abbott *et al.* (LIGO Scientific Collaboration and Virgo Collaboration), GW190521: A binary black hole merger with a total mass of 150 $M_{\bigodot}$, Phys. Rev. Lett. **125**, 101102 (2020).

[11] R. Abbott *et al.*, GW190814: Gravitational waves from the coalescence of a 23 solar mass black hole with a 2.6 solar mass compact object, The Astrophysical Journal **896**, L44 (2020).

[12] K. S. Stelle, Renormalization of higher-derivative quantum gravity, Phys. Rev. D **16**, 953 (1977).

[13] J. Meidam, K. W. Tsang, J. Goldstein, M. Agathos, A. Ghosh, C.-J. Haster, V. Raymond, A. Samajdar, P. Schmidt, R. Smith, K. Blackburn, W. Del Pozzo, S. E. Field, T. Li, M. Pürrer, C. Van Den Broeck, J. Veitch, and S. Vitale, Parametrized tests of the strong-field dynamics of general relativity using gravitational wave signals from coalescing binary black holes: Fast likelihood calculations and sensitivity of the method, Phys. Rev. D **97**, 044033 (2018).

[14] S. Khan, S. Husa, M. Hannam, F. Ohme, M. Pürrer, X. J. Forteza, and A. Bohé, Frequency-domain gravitational waves from nonprecessing black-hole binaries. ii. a phenomenological model for the advanced detector era, Phys. Rev. D **93**, 044007 (2016).

[15] S. Khan, K. Chatziioannou, M. Hannam, and F. Ohme, Phenomenological model for the gravitational-wave signal from precessing binary black holes with two-spin effects, Phys. Rev. D **100**, 024059 (2019).

[16] M. Hannam, P. Schmidt, A. Bohé, L. Haegel, S. Husa, F. Ohme, G. Pratten, and M. Pürrer, Simple model of complete precessing black-hole-binary gravitational waveforms, Phys. Rev. Lett. **113**, 151101 (2014).

[17] S. Husa, S. Khan, M. Hannam, M. Pürrer, F. Ohme, X. J. Forteza, and A. Bohé, Frequency-domain gravitational waves from nonprecessing black-hole binaries. i. new numerical waveforms and anatomy of the signal, Phys. Rev. D **93**, 044006 (2016).

[18] T. G. F. Li, *Extracting Physics from Gravitational Waves: Testing the Strong-field Dynamics of General Relativity and Inferring the Large-scale Structure of the Universe*, Ph.D. thesis, Vrije U., Amsterdam (2013).

[19] A. Buonanno, B. R. Iyer, E. Ochsner, Y. Pan, and B. S. Sathyaprakash, Comparison of post-newtonian templates for compact binary inspiral signals in gravitational-wave detectors, Phys. Rev. D **80**, 084043 (2009).

[20] T. G. F. Li, W. D. Pozzo, S. Vitale, C. V. D. Broeck, M. Agathos, J. Veitch, K. Grover, T. Sidery, R. Sturani, and A. Vecchio, Towards a generic test of the strong field dynamics of general relativity using compact binary coalescence: Further investigations, Journal of Physics: Conference Series **363**, 012028 (2012).

[21] M. Agathos, W. Del Pozzo, T. G. F. Li, C. Van Den Broeck, J. Veitch, and S. Vitale, Tiger: A data analysis pipeline for testing the strong-field dynamics of general relativity with gravitational wave signals from coalescing compact binaries, Phys. Rev. D **89**, 082001 (2014).

[22] R. E. Kass and A. E. Raftery, Bayes factors, Journal of the American Statistical Association **90**, 773 (1995).

[23] G. Ashton, M. Hübner, P. D. Lasky, C. Talbot, K. Ackley, S. Biscoveanu, Q. Chu, A. Divakarla, P. J. Easter, B. Goncharov, F. H. Vivanco, J. Harms, M. E. Lower, G. D. Meadors, D. Melchor, E. Payne, M. D. Pitkin, J. Powell, N. Sarin, R. J. E. Smith, and E. Thrane, Bilby: A user-friendly bayesian inference library for gravitational-wave astronomy, The Astrophysical Journal Supplement Series **241**, 27 (2019).

[24] J. Veitch and A. Vecchio, Bayesian coherent analysis of in-spiral gravitational wave signals with a detector network, Phys. Rev. D **81**, 062003 (2010).

[25] J. Veitch, V. Raymond, B. Farr, W. Farr, P. Graff, S. Vitale, B. Aylott, K. Blackburn, N. Christensen, M. Coughlin, W. Del Pozzo, F. Feroz, J. Gair, C.-J. Haster, V. Kalogera, T. Littenberg, I. Mandel, R. O'Shaughnessy, M. Pitkin, C. Rodriguez, C. Röver, T. Sidery, R. Smith, M. Van Der Sluys, A. Vecchio, W. Vousden, and L. Wade, Parameter estimation for compact binaries with ground-based gravitational-wave observations using the lalinference software library, Phys. Rev. D **91**, 042003 (2015).

[26] M. Maggiore, *Gravitational Waves: Volume 1: Theory and Experiments* (Oxford University Press, 2007).

[27] M. Ruiz, M. Alcubierre, D. Núñez, and R. Takahashi, Multiple expansions for energy and momenta carried by gravitational waves, General Relativity and Gravitation **40**, 1705 (2008), arXiv:0707.4654 [gr-qc].